A Random Zero Vector Strategy based on Markov Chain for Induction Motor Drive

Xie Fang, Hang Bing, Kangkang Liang and Wenming Wu

***Abstract*—**Higher-order harmonics can affect the running performance of induction motor. For the problem, the change should be done from the harmonic spectrum distribution to proceed so that the output of the inverter harmonic components relatively evenly distributed in a wide band, so as to minimize noise. In this paper, based on the volt-second balance equation of traditional algorithm, the linear equations of the pulse time of switching devices in 3-phase upper arms are set up and solved, thus a simplified algorithm for SVPWM without coordinate transformation and sector judgment is proposed. Then, Markov chain algorithm is used to determine the zero vector distribution coefficient for the simplified algorithm. The simulation and experimental results verify the effectiveness of the proposed strategy on induction motor under different load.

***Keywords*—**random zero vector (RZV), Markov chain, induction motor (IM), space vector pulse width modulation (SVPWM).

I. INTRODUCTION

Increasing use of electrical motors in automotive and shipping industry leads to more attention to dynamic characteristic and acoustic noise. In variable-speed motors, acoustic noise caused by the supply current harmonics is usually further than friction, imbalance, and aerodynamic origin especially during motor starting process [1]. The standard SVPWM strategy presents cluster harmonics with very large amplitudes, particularly near the integer multiple switching frequencies. For these reasons, Random space vector modulation (RSVM) strategy has been proposed and studied to avoid whistling and EMI noise [2-3]. M.M.Bech [4] proposes a type of random PWM in which the center of a two or three phase pulse position is placed randomly in the modulation interval, compared with RLL PWM. Hamid Soltani [5] presents the effect of the symmetrical regularly sampled SVPWM and Random Modulation technique on the drive's input current interharmonic magnitudes. Lai and Chen [6] investigate several kinds of RPWM techniques from the viewpoint of efficiency and harmonic spreading. A. C. Binoj Kumar [7] proposes a random frequency which was done on the DSP to reduce acoustic noise through comparison of the open-loops and closed-loops.

There are three modulation strategies included in the existing simple RSVM (one random parameter) [8]: random switching frequency SVPWM [9], random zero vector SVPWM [10] and random pulse position SVPWM [11]. However, the spectrum of the random SVPWM strategy is extremely complicated due to the random coefficient, so it is difficult to accurately predict the harmonic amplitude that is a key index to assess the performance of a modulation strategy [12]. Therefore, questions remain as to how to design an efficient and effective random strategy and well as the impact on the dynamic characteristics of induction motor.

This paper is organized as follows. Section II discusses the simplified algorithm for space vector pulse width modulation to obtain the expression for the zero vector distribution coefficient. The principle of Markov chain Model is introduced in section III. Simultaneously, section III describes the operation of the random zero vector based on Markov chain Model and illustrates its development process. Section VI compares the performance of the standard modulation strategy and proposed strategy in this paper. The correctness and effectiveness of the proposed strategy are demonstrated by the simulation and experimental results. Finally, Section V concludes the paper.

II. DIGITAL IMPLEMENTATION OF SIMPLIFIED ALGORITHM FOR SPACE VECTOR PULSE WIDTH MODULATION

The topology of the standard three-phase three-wire two level inverter is used in induction controlling. U_{dc} is the DC link voltage. The upper power device state of the three phase device are S_a, S_b, S_c. '1' and '0' represent the on and off state respectively. The AC link three phase voltages are U_{AO}, U_{BO}, U_{CO}.

$$\begin{bmatrix} \frac{2}{3} & -\frac{1}{3} & -\frac{1}{3} \\ -\frac{1}{3} & \frac{2}{3} & -\frac{1}{3} \\ -\frac{1}{3} & -\frac{1}{3} & \frac{2}{3} \end{bmatrix} \begin{bmatrix} S_a \\ S_b \\ S_c \end{bmatrix} = \frac{1}{U_{dc}} \begin{bmatrix} U_{AO} \\ U_{BO} \\ U_{CO} \end{bmatrix} \quad (1)$$

The three-phase voltage can be converted to two-phase voltage using Clark's transformation as Formula (2).

This work was supported by Key project of National Natural Science funds (51637001), National Natural Science Foundation of China (51607002), Natural Science Foundation of Anhui Province (1708085ME131) and Doctoral Scientific Research Foundation of Anhui University (J01001961).

Xie Fang is with the Department of school of Electrical Engineering and Automation, Anhui University, Hefei230601, Anhui, China (corresponding author; e-mail: 103336547 @qq.com).

Hang Bing is with the Department of Hangzhou hikvision digital technology co.,1td, Hangzhou310000, Zhejiang, China.

Kangkang Liang is with the Department of National Engineering Laboratory of Energy-Saving Motor & Control Technology, Anhui University, Hefei230601, China.

Wenming Wu is with the Department of Anhui Province Laboratory of Industrial Energy-Saving and Safety, Anhui University, Hefei230601, Anhui,China.

$$\begin{bmatrix} U_\alpha \\ U_\beta \end{bmatrix} = \frac{2}{3}\begin{bmatrix} 1 & -\frac{1}{2} & -\frac{1}{2} \\ 0 & \frac{\sqrt{3}}{2} & -\frac{\sqrt{3}}{2} \end{bmatrix}\begin{bmatrix} U_a \\ U_b \\ U_c \end{bmatrix} \quad (2)$$

Where U_α and U_β are variables in $\alpha\beta$ coordinate. U_a, U_b, U_c are variables in *abc* coordinate.

In *abc* and $\alpha\beta$ coordinate, the same voltage vector has different coordinate. Standard SVPWM algorithm could solve it for Formula (3) in $\alpha\beta$ coordinate, such as T_A, T_B, T_C.

$$V_{ref} = V_m T_m / T_s + V_n T_n / T_s \quad (3)$$

Where T_s is sampling time. T_m and T_n are response time of V_m and V_n in a sampling time.

Because of the three-phase reference voltage containing asymmetric components, using zero-sequence component $U_{0r} = (U_{Ar} + U_{Br} + U_{Cr})/3$, Formula (3) can be resolved to Formula (2) in *abc* coordinate.

$$\begin{bmatrix} U_{Ar} \\ U_{Br} \\ U_{Cr} \end{bmatrix} - \begin{bmatrix} U_{0r} \\ U_{0r} \\ U_{0r} \end{bmatrix} = \begin{bmatrix} U_{AOm} \\ U_{BOm} \\ U_{COm} \end{bmatrix}\frac{T_n}{T_s} + \begin{bmatrix} U_{AOn} \\ U_{BOn} \\ U_{COn} \end{bmatrix}\frac{T_n}{T_s} \quad (4)$$

Where U_{Ar}, U_{Br}, U_{Cr} are the three phase reference voltages.

According to the standard SVPWM algorithm, the pulse time of the upper power device T_A, T_B, T_C can be solved by Formula (5).

$$\begin{bmatrix} T_A & T_B & T_C \end{bmatrix}^T = S_m \bullet T_m + S_n \bullet T_n + S_7 \bullet T_7 \quad (5)$$

Using Formula (1), (4) and (5), Formula (6) can be gotten.

$$\begin{bmatrix} \frac{2}{3} & -\frac{1}{3} & -\frac{1}{3} \\ -\frac{1}{3} & \frac{2}{3} & -\frac{1}{3} \\ -\frac{1}{3} & -\frac{1}{3} & \frac{2}{3} \end{bmatrix}\begin{bmatrix} T_A \\ T_B \\ T_C \end{bmatrix} = \frac{T_S}{U_{dc}}\left(\begin{bmatrix} U_{Ar} \\ U_{Br} \\ U_{Cr} \end{bmatrix} - \begin{bmatrix} U_{0r} \\ U_{0r} \\ U_{0r} \end{bmatrix}\right) \quad (6)$$

Because of rank $\begin{bmatrix} \frac{2}{3} & -\frac{1}{3} & -\frac{1}{3} \\ -\frac{1}{3} & \frac{2}{3} & -\frac{1}{3} \\ -\frac{1}{3} & -\frac{1}{3} & \frac{2}{3} \end{bmatrix}$=2<3, Formula (6) could have infinite solutions.

$U_{\max}$ is the maximum value among U_{Ar}, U_{Br}, U_{Cr} while $U_{\min}$ the minimum value. Formula (7) is the solution of Equation (6).

$$\begin{bmatrix} T_A \\ T_B \\ T_C \end{bmatrix} = \frac{T_s}{U_{dc}}\left(\begin{bmatrix} U_{Ar} - U_{\min} \\ U_{Br} - U_{\min} \\ U_{Cr} - U_{\min} \end{bmatrix} + k\begin{bmatrix} 1 \\ 1 \\ 1 \end{bmatrix}\right) \quad (7)$$

Where k is the linear coefficient for fundamental solution.

$T_{\max}$ is the maximum value among T_A, T_B, T_C while $T_{\min}$ the minimum value. From the Figure 1, Formula (8) is given in any section. T_0 and T_7 are response time of V_0 and V_7.

$$\begin{cases} T_{\max} = T_m + T_n + T_7 \\ T_{\min} = T_7 \end{cases} \quad (8)$$

Otherwise

$$\begin{cases} T_7 = k_0(T_s - T_m - T_n), k_0 \in [0,1] \\ T_0 = (1-k_0)(T_s - T_m - T_n), k_0 \in [0,1] \end{cases} \quad (9)$$

Where k_0 is the zero-vector distribution variable.

From Formula (8) and (9), Formula (10) can be given.

$$T_{\max} + \frac{1-k_0}{k_0}T_{\min} = T_s \quad (10)$$

Considering Formula (7), the linear coefficient k can be obtained by Formula (11).

$$k = k_0(U_{dc} - U_{\max} + U_{\min}) \quad (11)$$

Using Formula (11) and (7), T_A, T_B and T_C could be gotten to control the power device. Usually, let $k_0 = 0.5$ in some standard SVM. Actually, the zero vector can be obtained by random strategy in Random space vector modulation (RSVM). This paper proposed the Markov chain Model and illustrated with a case study.

III. Random Space Vector Modulation Based on Markov Chain

The Markov chain model is a random process, in this model the transitions takes place from one state to another. The probability of the next state depends only on the current state. A Markov chain is a sequence of random variables X1, X2, X3, ... with the Markov property, namely that, given the present state, the future and past states are independent. Formally,

$$\begin{aligned} &P_r\left(X_{n+1} = x \middle| X_1 = x_1, X_2 = x_2, \cdots X_n = x_n\right) \\ &= P_r\left(X_{n+1} = x \middle| X_n = x_n\right) \end{aligned} \quad (12)$$

It is assumed that the transition among the different models obeys the Markov chain of finite state, and the structure of Markov chain is shown in Fig. 1.

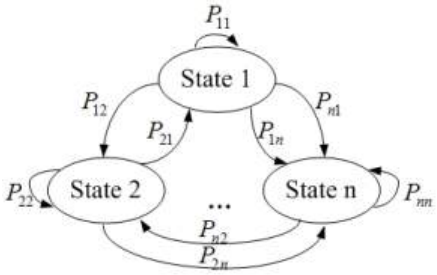

Fig. 1. Structure of the Markov chain

Fig. 2 shows a simple two-state Markov-Chain.

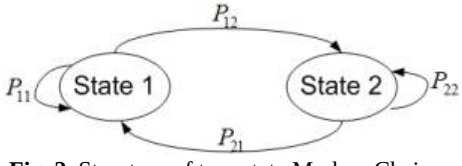

Fig. 2. Structure of two-state Markov Chain

The probability matrices of Markov chain can be described by Formula (13) in this paper.

$$P=\begin{bmatrix} P_{11} & P_{12} \\ P_{21} & P_{22} \end{bmatrix}=\begin{bmatrix} 1-P_t & P_t \\ P_t & 1-P_t \end{bmatrix} \quad (13)$$

Markov chain algorithm is used to determine the zero vector distribution coefficient k_0 for the simplified algorithm. The Simulink model of the two states Markov chain for IM is shown in Fig.3.

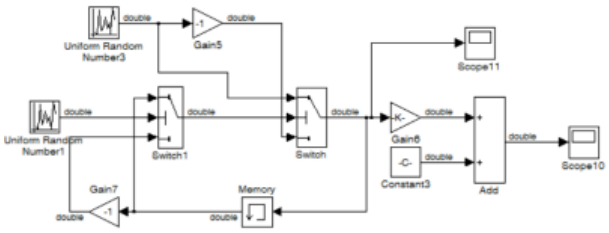

Fig. 3. Simulink model of two-state Markov Chain

IV. Simulation and Experiments

A. Simulation Results

To demonstrate the efficiency of the proposed random zero vector strategy, simulations for IM drive have been performed. The parameters of IM used in simulation are given as: rated power $P_N=1.1kW$, rated voltage $U_N=380V$,rated frequency $f_N=50Hz$, number of pole $P=2$, stator resistance $R_S=5.32\Omega$, stator leakage inductance $L_S=0.026H$, rotor resistance $R_r=5.49\Omega$, rotor leakage inductance $L_r=0.026H$, mutual inductance $L_m=0.361H$, moment of inertia $J=0.05kg\bullet m^2$. The IM system under two modulation strategies, i.e., fixed zero-vector distribution variable modulation which is called standard modulation in this paper and the proposed random zero vector strategy. The experiments are performed under no-load, low-load and heavy-load, respectively.

Case 1: Giving rotor speed is $n=1200r/\min$, in case of no-load starting up.

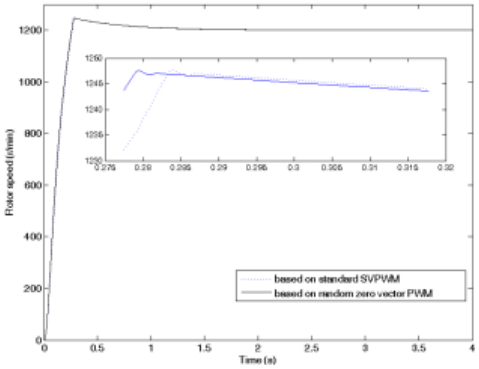

(a) Waveform of rotor speed

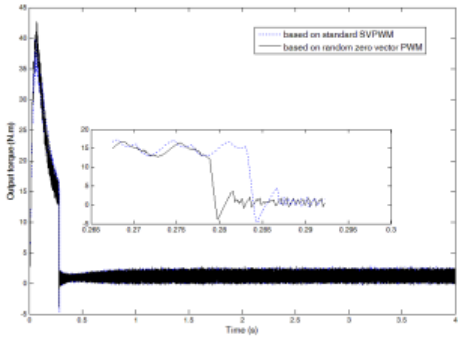

(b) Waveform of output torque

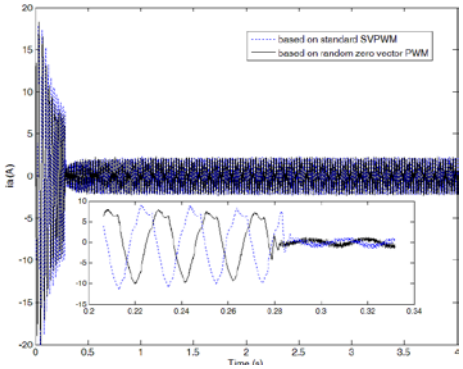

(c)Waveform of current i_a

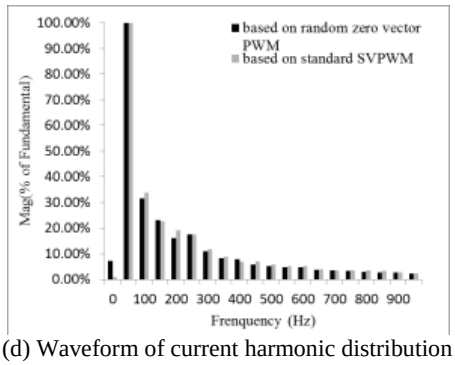

(d) Waveform of current harmonic distribution

Fig.4. Comparison waveform between standard SVPWM and new random zero vector SVPWM under no load

Through the FFT calculation, the total fundamental (50Hz)=10.92, the total harmonic distortion (THD)=51.45% using the new random zero vector PWM and the total fundamental (50Hz)=11.19, THD=54.31% using the standard SVPWM in Fig.4(d).

Case 2: Giving rotor speed is $n=1200r/\min$, in case of low-load starting up.

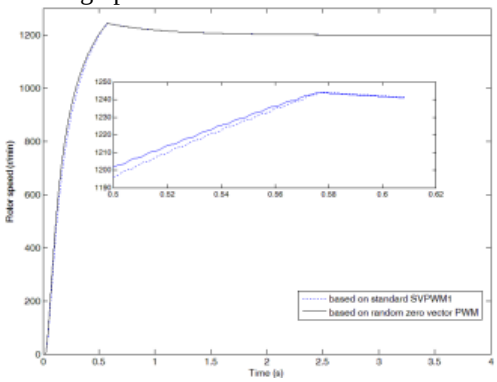

(a) Waveform of rotor speed

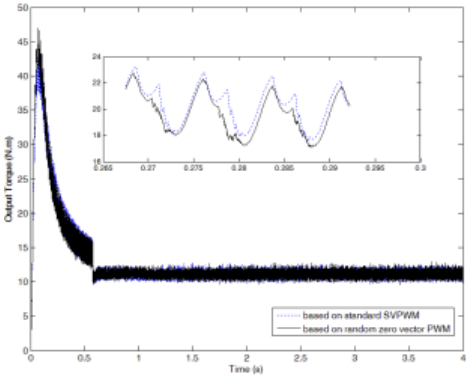

(b) Waveform of output torque

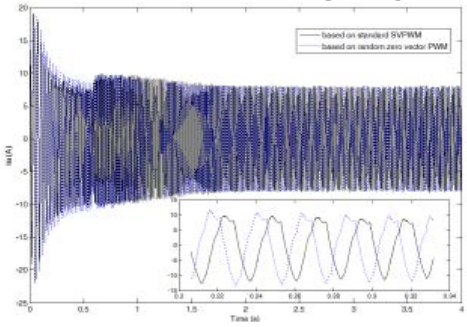

(c) Waveform of current i_a

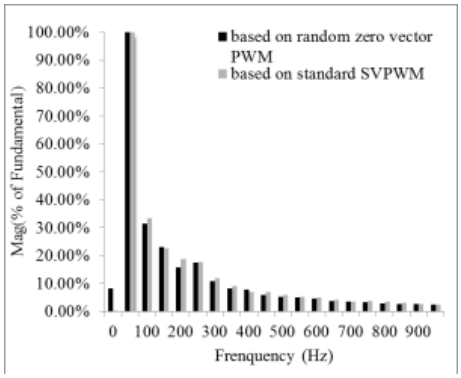

(d) Waveform of current harmonic distribution

Fig.5. Comparison waveform between standard SVPWM and new random zero vector SVPWM under low load

Through the FFT calculation, the total fundamental (50Hz)=10.91, THD=50.98% using the new random zero vector SVPWM and the total fundamental (50Hz)=11.16, THD=53.97% using the standard SVPWM in Fig.5(d).

Case3: Giving rotor speed is $n = 1200r/\min$, in case of heavy-load starting up.

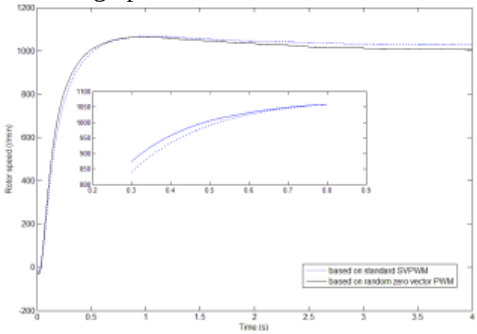

(a) Waveform of rotor speed

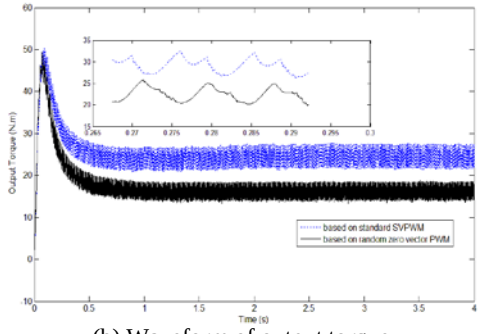

(b) Waveform of output torque

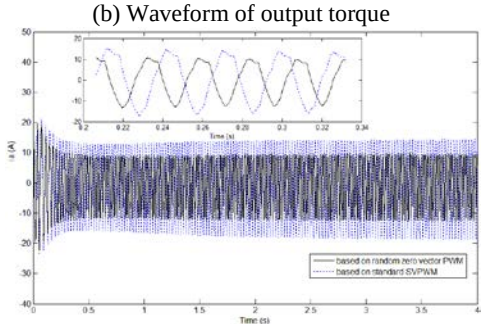

(c) Waveform of current i_a

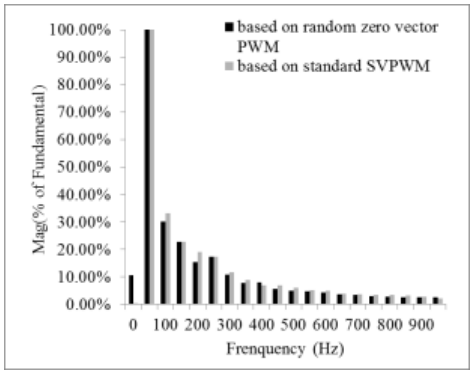

(d) Waveform of current harmonic distribution

Fig.6. Comparison waveform between standard SVPWM and new random zero vector SVPWM under heavy-load

Through the FFT calculation, the total fundamental (50Hz)=10.88, THD=49.82% using the new random zero vector PWM and the total fundamental (50Hz)=11.22, THD=53.90% using the standard SVPWM in Fig.6(d).

Fig.4-6 show that the new random zero vector control based on Markov chain algorithm can obviously reduce the higher harmonic current but not affect the fundamental harmonic under different loads. The bigger the load torque is, the smaller the value of THD. The results validate the control strategy improve effectively the response speed and the output torque, tracks fast to the setting values from the start to stability especially. It also shows that the amplitude of the three-phase currents decreased. Simulation results demonstrate that the proposed modulation not only has a fast response, reduces the harmonic under motor start conditions, but also could not be affected by the parameter variations of motor and inverter.

B. Experimental Results

The experimental setup of the IM drive consists of the induction motor, an incremental photoelectric encode, and two current sensors. The system is controlled by PC using a semi-physical simulation platform based on Applied Dynamics

International (ADI) in real-time simulation and control. The ADI is equipped with data input and output board, analogue input and output board, encode-pulse board and supported by Advantage software. All of the data from sensors as well as the controllers are written in the Simulink mode to calculate. Fig.7 shows the test bench.

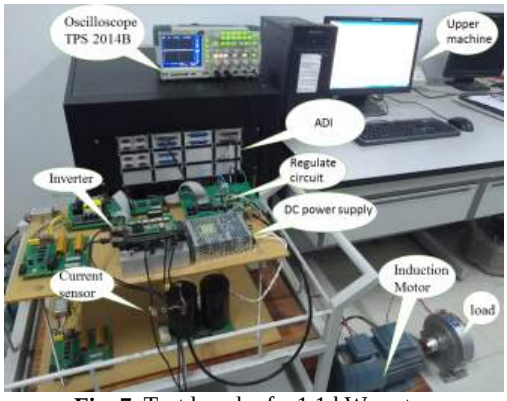

Fig. 7. Test bench of a 1.1 kW motor

Both the standard modulation and the proposed modulation are used to get the current harmonic distribution of the above-mentioned induction motor. The comparative experiments are studied for induction motor of no load, low load, medium load and heavy load starting up.

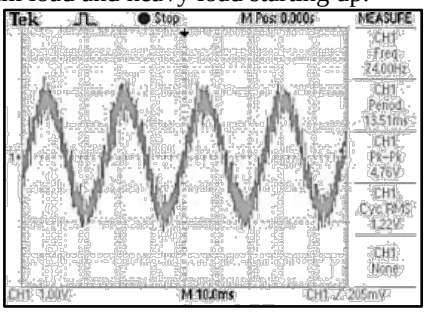

(a) Waveform of current i_a using Standard SVPWM

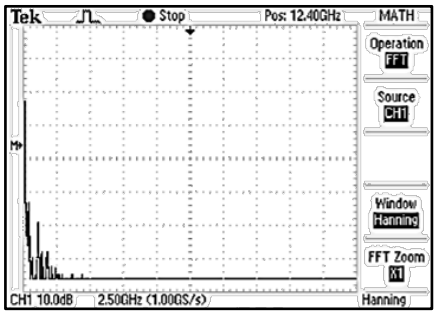

(b) Waveform of current harmonic distribution using Standard SVPWM

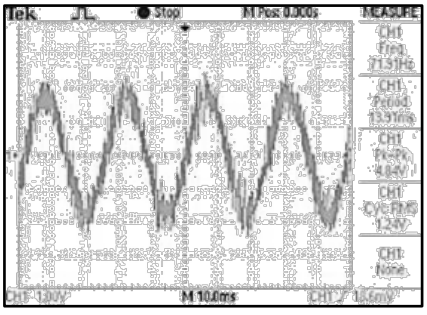

(c) Waveform of current i_a using the proposed random zero vector SVPWM

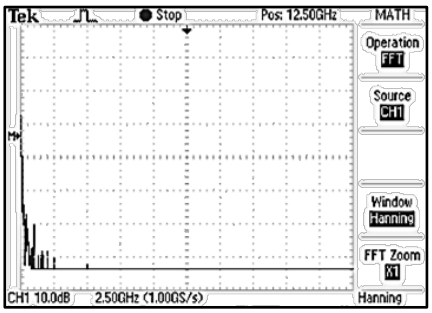

(d) Waveform of current harmonic distribution using the proposed random zero vector SVPWM

Fig.8. Comparison of two modulation strategies under no load

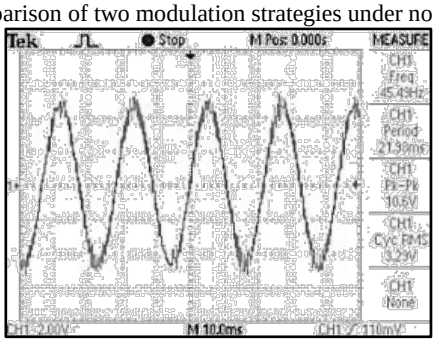

(a) Waveform of current i_a using Standard SVPWM

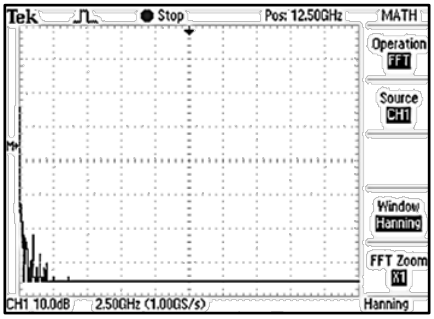

(b) Waveform of current harmonic distribution using Standard SVPWM

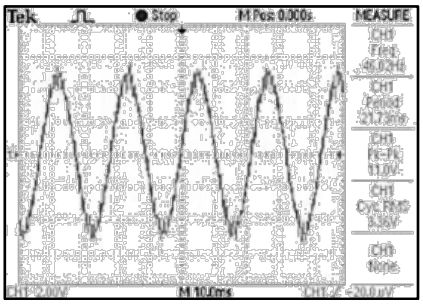

(c) Waveform of current i_a using the proposed random zero vector SVPWM

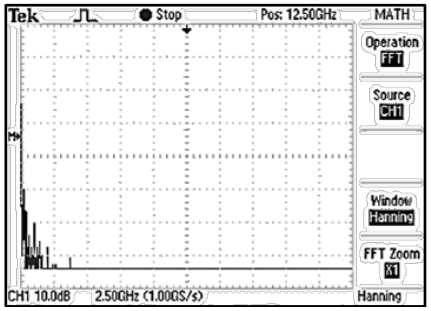

(d) Waveform of current harmonic distribution using the proposed random zero vector SVPWM

Fig.9. Comparison of two modulation strategies under low load

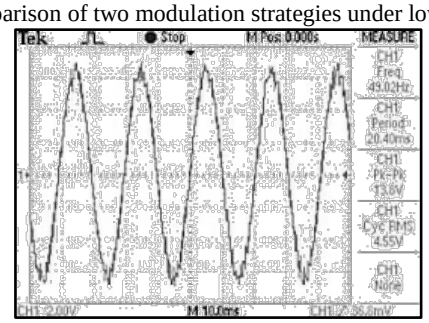

(a) Waveform of current i_a using Standard SVPWM

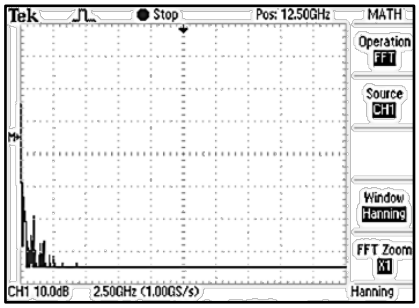

(b) Waveform of current harmonic distribution using Standard SVPWM

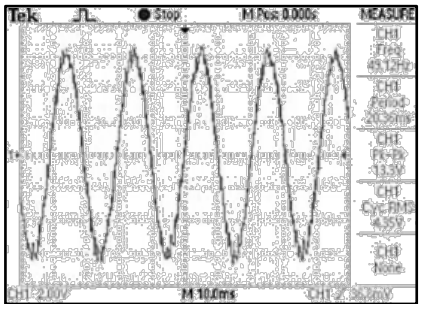

(c) Waveform of current i_a using the proposed random zero vector SVPWM

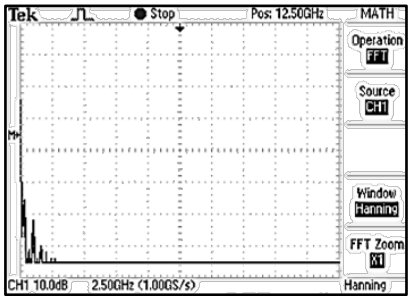

(d) Waveform of current harmonic distribution using the proposed random zero vector SVPWM

Fig.10. Comparison of two modulation strategies under medium load

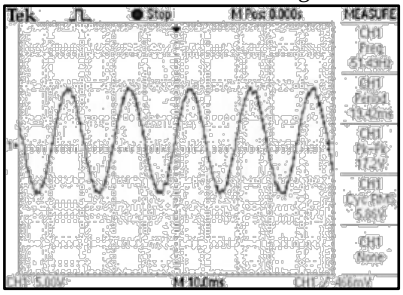

(a) Waveform of current i_a using Standard SVPWM

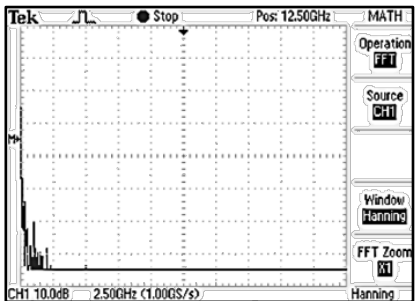

(b) Waveform of current harmonic distribution using Standard SVPWM

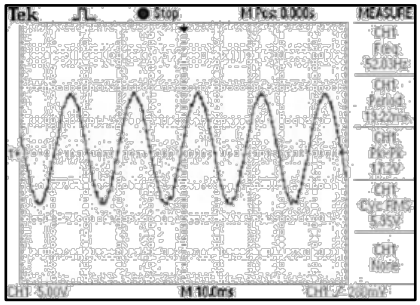

(c) Waveform of current i_a using the proposed random zero vector SVPWM

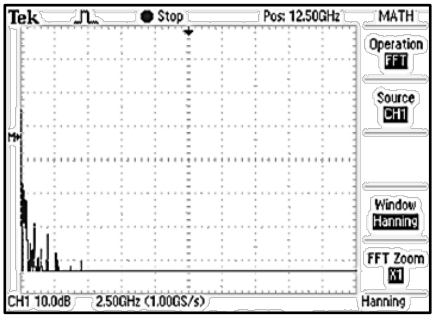

(d) Waveform of current harmonic distribution using the proposed random zero vector SVPWM

Fig.11. Comparison of two modulation strategies under heavy load

Some experimental results presented under different load in Fig.8-11 in this chapter, and the simulation results as well, point out the promising features and characteristics of the proposed strategy applied to induction motor drives. The proposed strategy can effectively distribute uniformly the harmonic spectrum especially near the fundamental frequency and its multiples in radio frequency range.

V. CONCLUSIONS

The random zero vector strategy for IMs based on Markov Chain has been proposed in this paper. The correction and the effectiveness of the proposed strategy have been verified at an IM drive. The experimental results demonstrate that the strategy can effectively distribute uniformly the harmonic spectrum so that the output of the inverter harmonic components relatively evenly distributed in a wide band, so as to minimize noise. Moreover, compared with standard modulation, the real-time implementation of the proposed random zero vector strategy can ensure the output waveform of current quality, and reduce THD obviously, especially under heavy load. At the same time, the advantage of the highest DC

voltage utilization ratio of standard SVPWM is inherited. In conclusion, the proposed modulation can be widely applied to all kinds of the variable speed system and its popularization.

REFERENCES

[1] M. A. Hannan, Jamal Abd Ali, Azah Mohamed, and Mohammad Nasir Uddin, "A random forest regression based Space Vector PWM inverter controller for the induction motor drive", *IEEE Transactions on Industrial Electronics*, vol.64, no.4, pp. 2689 – 2699, 2017.

[2] Amir Peyghambari, Ali Dastfan; Alireza Ahmadyfard, "Selective voltage noise cancellation in three-phase inverter using random SVPWM", *IEEE Transactions on Power Electronics*, vol.31, no.6, pp. 4604 – 4610, 2016.

[3] B. Jacob and M. Baiju, "Spread spectrum modulation scheme for twolevel inverter using vector quantised space vector-based pulse density modulation", *IET Electr. Power Appl*, vol. 5, pp. 589–596, 2011.

[4] M.M.Bech, J.K.Pedersen, and F. Blaabjerg, "Random modulation techniques with fixed switching frequency for three-phase power converters", *IEEE Transactions on Power Electron*, vol.15, no.4, pp. 753-761, 2000.

[5] Hamid Soltani, Pooya Davari, Firuz Zare, and Frede Blaabjerg, "Effects of modulation techniques on the input current interharmonics of Adjustable Speed Drives", *IEEE Transactions on Industrial Electronics*, vol.65, no.1, pp.167-178, 2018.

[6] Y.-S. Lai and B.-Y. Chen, "New random PWM technique for a full-bridge DC/DC converter with harmonics intensity reduction and considering efficiency", *IEEE Transactions on Power Electron*, vol.28, no.11, pp. 5013–5023, 2013.

[7] A. C. Binoj Kumar and G. Narayanan, "Variable-Switching Frequency PWM Technique for Induction Motor Drive to Spread Acoustic Noise Spectrum With Reduced Current Ripple", *IEEE Transactions on Industry applications*, vol.52, no.5, pp. 3927 - 3938, 2016.

[8] Boudouda Aimad, Boudjerda Nasserdine, El Khamlichi Drissi Khalil, Kerroum, and Kamal, "Combined random space vector modulation for a variable speed drive using induction motor", *Electrical Engineering*, vol.98, no.1, pp. 1-15, 2016.

[9] Hamid Khan, El-Hadj Miliani, and Khalil El Khamlichi Drissi, "Discontinuous random space vector modulation for electric drives: A digital approach", *IEEE Transactions on Power Electronics*, vol.27, no.12, pp. 4944 – 4951, 2012.

[10] Seung-Yeol Oh, Young-Gook Jung, Seung-Hak Yang, Young-Cheol Lim, "Harmonic-Spectrum spreading effects of two-phase random centered distribution PWM (DZRCD) scheme with dual zero vectors", *IEEE Transactions on Industrial Electronics*,vol.56, no.8, pp. 3013 – 3020, 2009.

[11] S. -H. Na, Y. -G. Jung, Y. -C. Lim, S. -H. Yang, "Reduction of audible switching noise in induction motor drives using random position space vector PWM", *IEE Proceedings - Electric Power Applications*, vol. 149, no.3, pp.195-200, 2002.

[12] Guoqiang Chen, Jianli Kang, "Frequency spectrum customization and optimization by using Monte Carlo method for random space vector pulse width modulation strategy", *International Journal of Signal Processing, Image Processing and Pattern Recognition*, vol.9, no.12, pp. 135-152,2016.

Xie Fang was born on Dec. 20, 1977. She received the PhD degree in Circuits and Systems from Anhui University of China. Currently, she is a researcher at school of Electrical engineering and automation, Anhui University, China. Her major research interests include motor controlling and power electronic technology. She has published many papers in related journals. In addition, she has worked at postdoctoral research station in Hefei Hengda Jianghai Pump Co., Ltd in in recent years.

Hang Bing was born on Feb.28, 1990. Currently, he works at Hangzhou hikvision digital technology co.,1td, Hangzhou, Zhejiang, China. His major research interest is motor controlling .

Kangkang Liang was born on Mar.2, 1994. Currently, he is a graduate student at school of Electrical engineering and automation, Anhui University, China. His major research interest is motor controlling.

Wenming Wu was born on sept.13, 1992. Currently, he is a graduate student at school of Electrical engineering and automation, Anhui University, China. His major research interest is motor controlling.